

Physics-informed two-stage neural network enables computational ghost imaging through unknown scattering media

Cite as: Appl. Phys. Lett. **127**, 071103 (2025); doi: [10.1063/5.0283491](https://doi.org/10.1063/5.0283491)

Submitted: 1 June 2025 · Accepted: 30 July 2025 ·

Published Online: 18 August 2025





View Online



Export Citation



CrossMark

Zhengqing Gao,¹  Xiaoyan Wu,^{1,a)} Xinliang Zhai,¹ Ze Zheng,¹  Jianhong Shi,¹ Jingzheng Huang,^{1,2,3,a)} and Guihua Zeng^{1,2,3}

AFFILIATIONS

¹State Key Laboratory of Photonics and Communications, Center for Quantum Sensing and Information Processing, School of Electronic Information and Electrical Engineering, Shanghai Jiao Tong University, Shanghai 200240, China

²Shanghai Research Center for Quantum Sciences, Shanghai 201315, China

³Hefei National Laboratory, Hefei 230088, China

^{a)}Authors to whom correspondence should be addressed: xiaoyanwu@sjtu.edu.cn and jzhuang1983@sjtu.edu.cn

ABSTRACT

Imaging through scattering media located behind and in front of the object simultaneously remains a significant challenge in computational ghost imaging, as the reconstructed images are often severely degraded due to distorted illumination patterns and attenuated intensity values. In this Letter, we propose an untrained, two-stage self-supervised neural network that effectively mitigates both forward and backward scattering effects. Without the need for any labeled training data, our physics-informed framework exhibits strong adaptability to various types of unknown scattering media. We experimentally demonstrate the robustness of the proposed method by imaging through different scattering environments, including biologically relevant media and rotating ground glass. Compared with the existing reconstruction algorithms, our approach achieves substantially improved image quality for computational ghost imaging in unknown scattering media. This study introduces a paradigm for imaging through complex media and paves the way toward practical applications in biomedical and remote sensing scenarios.

Published under an exclusive license by AIP Publishing. <https://doi.org/10.1063/5.0283491>

The application scenarios of imaging through scattering media are diverse, such as underwater imaging (through the water),^{1–3} navigation in foggy conditions (through the atmosphere),^{4,5} and bioimaging (through skin or human tissue).^{6–8} However, the absorption and scattering caused by scattering media can significantly affect the SNR of the target. Accordingly, imaging through thick scattering media has been repeatedly identified as one of the most important open problems in optics.^{8,9}

Traditional imaging methods based on geometric optics are ineffective when dealing with disordered light beams under scattering conditions. However, advancements in optoelectronic devices and computational techniques have facilitated the development of imaging methods for visualizing objects through scattering media. To achieve more precise tracking and manipulation of light, researchers have developed various methods, such as through speckle correlation,¹⁰ waveform control in the terahertz band,^{11–13} noninvasive imaging,¹⁴ and design of optical materials.¹⁵ Recent advances in the synergistic

integration of material innovations with single-pixel imaging methodologies¹⁶ have overcome the inherent limitations of conventional detection systems in multi-wavelength information retrieval under complex environmental conditions. However, relying on single-pixel imaging algorithms still leads to difficulties in dealing with forward scattering when the scattering medium is located in front of the object. Therefore, although these techniques provide valuable solutions, their limitations highlight the need for innovative approaches to overcome the challenges of imaging through scattering media.

In recent years, with the rapid development of digital technology, big data, and advanced optoelectronic technologies, deep learning (DL) has demonstrated significant potential in the fields of optics and photonics.^{17,18} Recently, Peng and Chen proposed a two-stage framework¹⁹ that integrates a supervised correction network with an unsupervised denoising network. The supervised network was trained using simulated data, achieving enhanced contrast and spatial resolution in dynamic scattering environments. However, supervised learning

methods often require large amounts of training data, and extracting universal information from speckle patterns under highly degraded conditions remains a substantial challenge. Moreover, purely data-driven DL methods tend to exhibit limited generalization capabilities due to their heavy reliance on training data. Researchers have developed various approaches to tackle this issue. The unsupervised deep learning (UnDL)²⁰ enables high-quality object imaging under noise interference and low sampling rate conditions. The algorithm combines a physical imaging module with a deep learning enhancement module to construct an unsupervised learning framework, enabling high-quality real-time image reconstruction under low sampling rates and high-noise conditions without requiring clean training data, while integrating noise robustness and high frame rate capabilities. Furthermore, ghost imaging with deep neural network constraint (GIDC)²¹ achieves super-diffraction-limited resolution in far-field imaging by embedding the physical image formation model of ghost imaging into a deep neural network framework. However, these algorithms often account only for backward scattering while neglecting forward scattering effects in scattering scenarios. Furthermore, relying solely on 1D intensity signals without incorporating additional priors may further amplify uncertainties in the imaging process.

We employ a two-dimensional detector instead of a single-pixel detector to capture the raw images during the experiment. The bucket detection value sequence can be calculated by summing all pixels' values of each image, which is subsequently used to conduct loss1 and loss2 in our proposed algorithm. Additionally, the two-dimensional images collected by the array detector can provide extra prior information for the network, thereby mitigating the effects of forward scattering. For image reconstruction, we design a self-supervised neural network. This network consists of two parts, each dedicated to learning the transmission matrix for forward and backward scattering, respectively. A self-supervised model based on physical priors can address the generalization issues in different scattering scenarios, reducing the dependency on data and significantly improving feature extraction efficiency. An efficient physical prior can offer optimized guidance to identify the best reconstruction solution across various scattering scenarios. Notably, the network is optimized by computing the loss between the reconstructed image and the collected image, eliminating the need for extensive training data. We conducted experiments using a variety of scattering media. The results show that, compared with ghost imaging methods, such as traditional ghost imaging (TGI),²² differential ghost imaging (DGI),²³ UnDL, and GIDC, this method achieves higher-quality image reconstruction and demonstrates strong adaptability in practical scenarios. This highlights the tremendous potential of physics-informed self-supervised neural networks.

In mathematics, we can use a transmission matrix T describe the relationship of the light field before (E_{in}) and after (E_{out}) passing through a scattering media, i.e.,

$$E_{out} = TE_{in}. \quad (1)$$

Here, the scattering media is described by a transmission matrix T , whose elements t_{ij} follow a complex Gaussian distribution^{24,25} with a zero mean and a variance σ . Measuring the transmission matrix is often time-consuming and labor-intensive, raising the important question of how to image through an unknown scattering media. The proposed algorithm utilizes a physics-based self-supervised network to generate high-quality and high-resolution results without measuring

the transmission matrix. Its inputs are the captured 2D speckle patterns I_N and the calculated corresponding intensity values s_N , which are easily obtainable in structured light illumination-based imaging. The schematic diagram of the imaging system is shown in Fig. 1(a). Parallel light is modulated by the digital micromirror device (DMD) and then incident on a target with scattering media on both the front and back sides. The original speckle pattern P_N modulated on the DMD is shown in Fig. 1(b). The light is then collected by a two-dimensional detector, and the captured image I_N is shown in Fig. 1(c). The corresponding intensity values s_N calculated from the image are shown in Fig. 1(d). The captured 2D images I_N and their corresponding 1D intensity values s_N are subsequently used as inputs to the network. After iterative optimization, high-quality and high-resolution results are obtained.

Our proposed network can be divided into two parts, W_1 and W_2 , dedicated to modeling the transmission matrices for forward and backward scattering, respectively. The complete algorithm overview is summarized in Algorithm 1 and in Fig. 2. Here, $G(x, y)$ represents the correlation operation and \odot represents the element-wise multiplication. The input to the network is the 2D detected speckle I_N , computed intensity values s_N , and modulation patterns P_N . We use a network to simulate the forward propagation process, generating patterns influenced by the forward scattering media, which are the patterns ultimately illuminating the object. By correlating these patterns with the collected intensity values, the target unaffected by forward scattering can be recovered. To efficiently train the network, we separately simulate the forward and backward propagation processes and compare the predicted results with the experimentally collected results, thereby updating the parameters of both networks.

To calculate the network loss, we first predict the target image to obtain predicted correlation results. Subsequently, we compute the loss by comparing the correlation results obtained from the collected signals with the predicted results, and then update the parameters in W_1 accordingly. Additionally, we obtain the predicted speckle image and compare them with the collected image to compute loss, updating the parameters in W_2 . Using the difference between these two predicted variables and the collected signal as loss of the network, the network parameters are trained. Through iterative network updates, the reconstructed image can be updated. This algorithm utilizes an encoder-decoder structure to reconstruct the object image from the intensity and corresponding 2D detected speckle. The network architecture we employ in this work was derived from the U-net.²⁶ It is worth noting that when using the proposed network, there are no restrictions on the depth and partition number of the neural network. Therefore, optimizing the depth and partition number of the neural network may result in better performance. In this work, the whole network plays the role of a solver for the optimization problem of computing inverse physical processes of imaging. The objective function can be formulated as

$$\min_{\theta} \frac{1}{M} \sum_k ||P * \mathcal{R}_{\theta}(I_k; P) - I_k||_2^2 + \tau \sum_x |\nabla \mathcal{R}_{\theta}(I_k; P)|, \quad (2)$$

where \mathcal{R}_{θ} denotes the proposed model and τ is a weighting factor. The first term of the function is the mean square error (MSE) between measurements and the speckle predictions. The second term is the

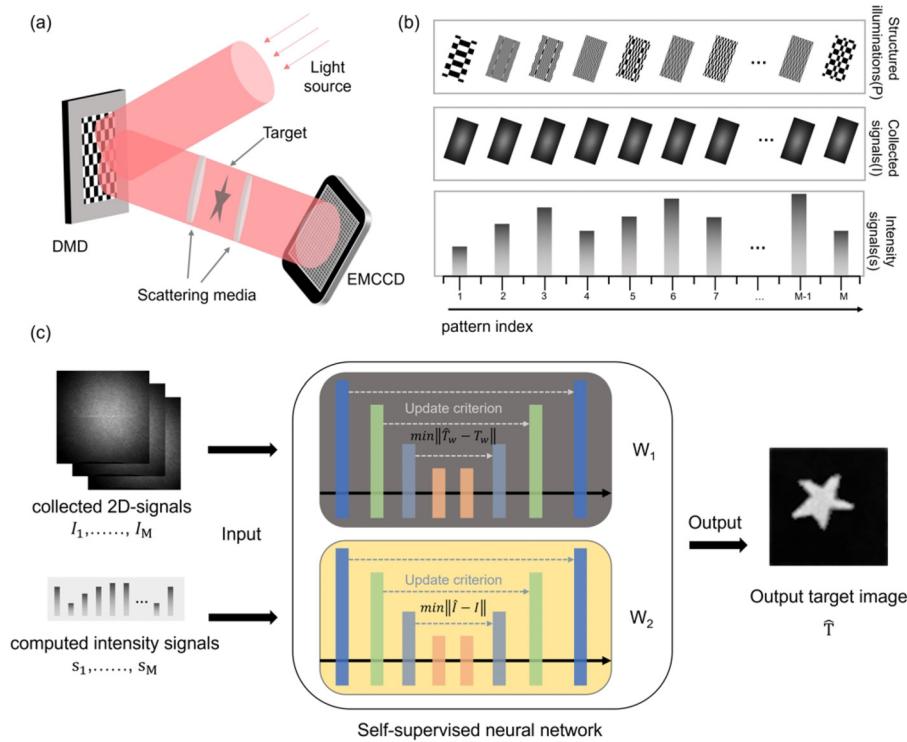


FIG. 1. Overview of the proposed algorithm. (a) Schematic diagram of the imaging system. Structured light is incident on a target with scattering media on both sides, and is subsequently collected by a camera. (b) Original speckle pattern P modulated by DMD, degraded speckle pattern I captured by camera, and corresponding intensity values calculated from I . (c) The overall workflow of the algorithm is presented.

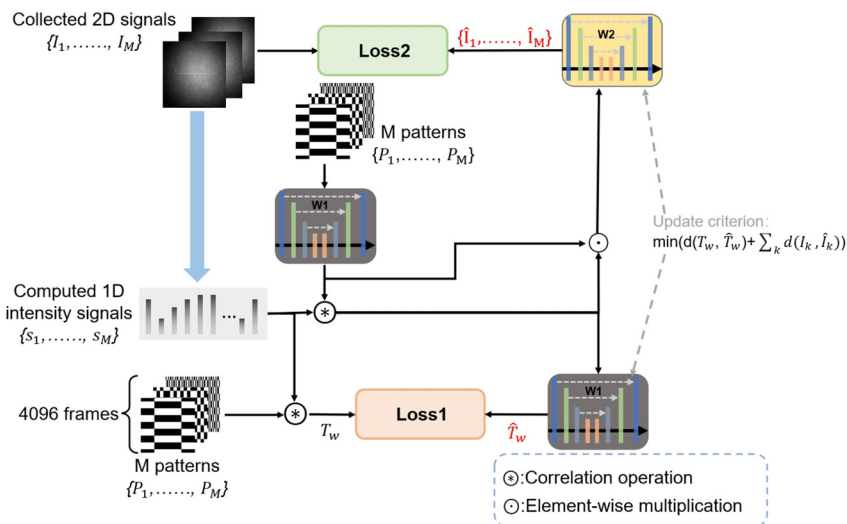


FIG. 2. Flow chart of the physics-informed learning method for scattering imaging.

total variation of the output image, which is beneficial for converging and improving the reconstruction results.

To demonstrate the practical effectiveness of the proposed algorithm, we conducted several experiments to evaluate its performance in the presence of unknown scattering media. In the later sections, the reconstructed results under different scattering media and different imaging algorithms will be presented in detail. In addition, we quantitatively assessed the quality of the retrieved images using the Pearson

correlation coefficient (PCC)²⁷ and structure similarity index measure (SSIM).²⁸ PCC indicates the strength of the linear relationship between two variables, with the absolute value of the coefficient representing the strength of the correlation; the larger the absolute value, the stronger the correlation. SSIM is a metric used to measure the structural similarity between two images, evaluating the image quality by comparing the luminance, contrast, and structural information of the images.

Algorithm 1. Proposed algorithm. We use default values learning rate α is 0.05, and the momentum β in the batch normalization is 0.6. The ReLU is used as the activation function for each layer. Generally speaking, the weighted factor of TV is set as $\tau=10^{-5}$, and convergence is achieved after about 200 iterations.

Input: $\{P_1, \dots, P_M\}, \{I_1, \dots, I_M\}, \{s_1, \dots, s_M\}$

Output: θ_1 of f_{w1} , θ_2 of f_{w2}

- 1: **Initialize:** θ_1 of f_{w1} , θ_2 of f_{w2}
- 2: **for** step = 1, 2, ..., N **do**
- 3: $\{\hat{P}_1, \dots, \hat{P}_M\} = f_{w1}(\{P_1, \dots, P_M\})$
- 4: $\hat{T} = G(\{\hat{P}_1, \dots, \hat{P}_M\}, \{s_1, \dots, s_M\})$
- 5: $\{\hat{I}_1, \dots, \hat{I}_M\} = f_{w2}(\{\hat{P}_1, \dots, \hat{P}_M\} \odot \hat{T})$
- 6: $\hat{T}_w = f_{w1}(\hat{T})$
- 7: $T_w = G(\{P_1, \dots, P_M\}, \{s_1, \dots, s_M\})$
- 8: Update θ_1 and θ_2 according to loss (\hat{T}_w, T_w) and loss $(\{\hat{I}_1, \dots, \hat{I}_M\}, \{I_1, \dots, I_M\})$
- 9: **end for**

The experimental setup is shown in Fig. 3(a). The light source is a pulsed laser with a power of 10 mW, equipped with a filter to a wavelength of $\lambda = 680$ nm. After collimation, the light is directed onto a DMD (DLC9500P24, 1080×1920) with pre-modulated patterns. The reflected light passes through a 4f system composed of two lenses, each with a focal length of 100 mm, and is projected onto the object with

scattering media on both the front and back sides. Finally, the light from the object is collected by another lens with a focal length of 100 mm and detected by a two-dimensional detector. The detector used in Figs. 4 and 7 is a CMOS (INOVANCE VC21-060GC-018, 3072×2048), while the detector employed in Fig. 5 is an EMCCD (Andor iXon Ultra 888, 1024×1024).

First, we utilized ground glass as scattering media to show the impact of scattering on imaging quality. As illustrated, Fig. 3(b) represents the image captured without the scattering media, Fig. 3(c) represents the image captured with the scattering media, and Fig. 3(d) compares the pixel values along the 100th row of Figs. 3(a) and 3(b). Without passing through the scattering media, we can see the image quite clearly. After passing through the scattering media, we can only see a speckle, and much of the information of the image is lost. It is evident that the presence of the scattering media significantly degrades the quality of the captured images, resulting in severe blurring and even making the images unrecognizable.

Next, we perform imaging on the same data using DGI, GIDC, UnDL, and our proposed method to demonstrate the superiority of our approach in image reconstruction. All comparison methods using the same input data and experimental conditions. Here, we select ground glass as the scattering media. DGI employs second-order operations to correlate light intensity and speckle images to generate images. Our proposed method embeds the physical model into the neural network, allowing better utilization of speckle information. UnDL performs denoising through an unsupervised network. However, when using a pre-trained unsupervised network for denoising, there may be

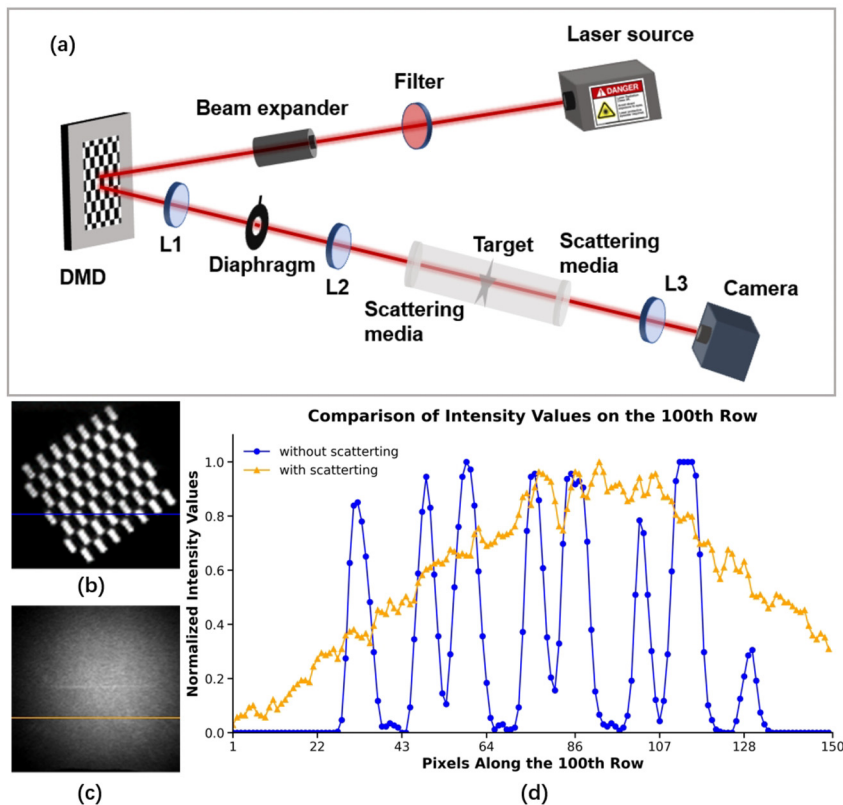


FIG. 3. Experimental optical setup. (a) Schematic diagram of the imaging system. (b) Scattering-free target image. (c) Scattering-affected target image. (d) Comparison of pixel values in the 100th row between these two images.

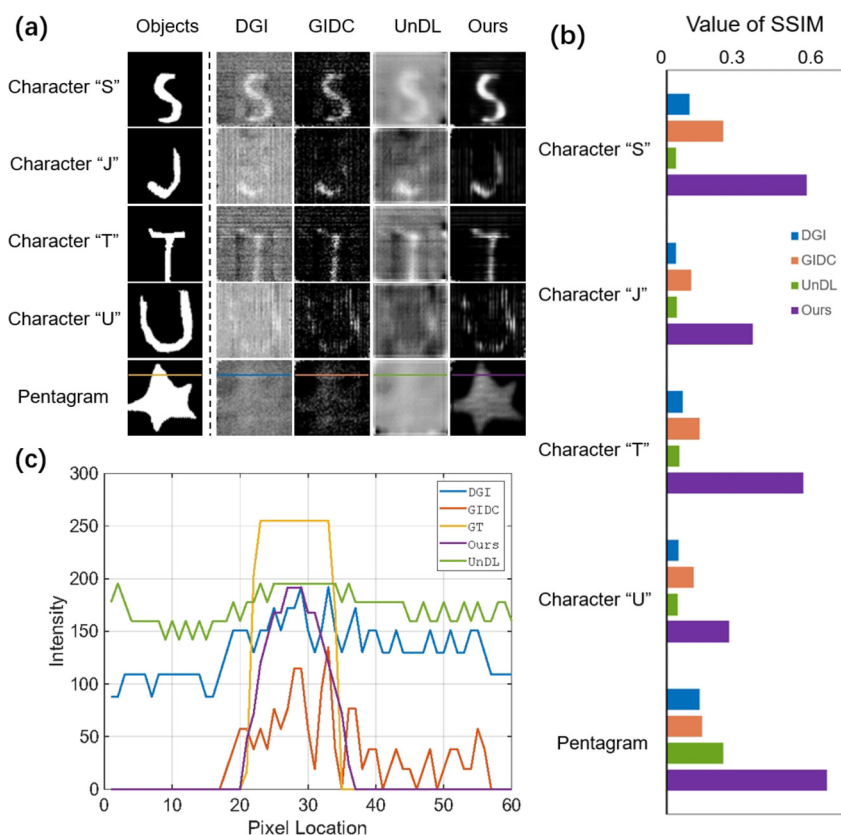


FIG. 4. Comparisons of DGI, GIDC, UnDL, and our method in the experiment. (a) Experimental results for different objects, where each row in each group represents the results reconstructed by different methods for the same object, and each column represents the results of different objects reconstructed by the same method. (b) Quantitative evaluation of the SSIM of the DGI, GIDC, UnDL, and ours. (c) Cross-sectional profile of solid line shown in (a).

issues such as poor generalization performance. GIDC integrates the physical model of GI formation into a deep neural network and does not require pre-training on any dataset. However, it overlooks the redundant information in the original speckle patterns, which will affect the quality of the retrieved ghost images. By comparing our

proposed method with these existing methods, we can observe its advantages in removing redundant information from speckle patterns and enhancing imaging quality.

Figure 4(a) shows images generated by different algorithms, with our method's output in the fifth column, exhibiting significantly reduced background noise and enhanced contrast. Using the same speckle patterns and data, DGI—though widely used—performs poorly in contrast and noise; UnDL achieves partial denoising but suffers from blurred artifacts and reduced resolution; GIDC, embedding physical models, shows improved performance but retains noticeable noise. In contrast, our results demonstrate superior spatial resolution, reduced noise across the entire image, and better contrast. Quantitatively, SSIM values [Fig. 4(b), with red, orange, green, and yellow lines representing our method, DGI, GIDC, and UnDL, respectively] confirm our method consistently achieves higher scores, indicating superior high-quality reconstruction capability. As further shown in Fig. 4(c), our reconstructed images also feature higher contrast with clean backgrounds. Compared to other methods, ours effectively utilizes collected information, eliminates redundant data that traditional GI struggles with, avoids dataset constraints of deep learning-based GI, saves training time, and achieves higher quality—enabling high-visibility, high-speed, high-quality image reconstruction without datasets.

Later, we conducted experiments with various unknown scattering media, and the experimental results are shown in Fig. 5. Here, we simulated scattering media that may appear in biomedical applications.

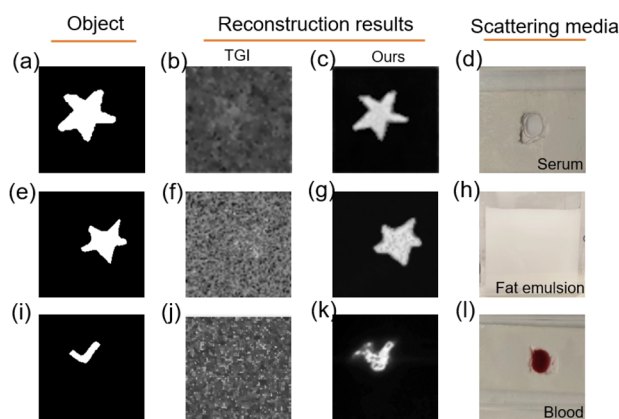


FIG. 5. Reconstructed results from various unknown scattering media. (a), (e), and (i) correspond to the target images; (b), (f), and (j) are the reconstructed results obtained by TGI; (c), (g), and (k) are the reconstructed results obtained by our method; (d), (h), and (l) represent the scattering media employed in this experiment.

Figures 5(a), 5(e), and 5(i) are the target images for imaging. Figures 5(b), 5(f), and 5(j) are the imaging results of TGI. Figures 5(c), 5(g), and 5(k) are the imaging results obtained by our method. Figures 5(d), 5(h), and 5(l) show the scattering media used in the imaging process. The scattering media employed in Figs. 5(a)–5(c) is serum, and the imaging target is a pentagram. Similarly, in Figs. 5(e)–5(g), the scattering media is fat emulsion, with the imaging target being a pentagram. The diffuser (DG10-120, Thorlabs) has a thickness of approximately 2 mm. Both the undiluted serum and blood have a thickness of about 1 mm. The fat emulsion solution is uniformly prepared by mixing 360 mm of de-ionized water and 0.4 mm of 20% concentration fat emulsion injection (6B300200020, Baxter) in a water tank container, which has a thickness of approximately 49.2 mm.

For Figs. 5(i), 5(j), and 5(k), the scattering media is blood, and the imaging target is a checkmark. It is observable that under the condition of this specific scattering media, TGI fails entirely to visualize the contour of the object. In contrast, our proposed method is capable of roughly reconstructing the shape of the object. Evidently, the experimental outcomes differ distinctly for each scattering media. Nevertheless, when compared with TGI, our method brings about a remarkable enhancement in image quality. This superiority holds true even in scenarios where traditional imaging algorithms are unable to display the object’s contours.

Subsequently, we evaluated the performance of the proposed algorithm in dynamic scattering scenarios. In the experiment, manually rotated ground glass was used as the scattering medium with a rotation speed of approximately 2.5°/s. A letter “S” target was imaged under these conditions, with colormap results from DGI, GIDC, UnDL, and our proposed method illustrated in Fig. 6(a). Figure 6(b) presents the PCC and SSIM performance metrics of these reconstructed images. As evidenced by the experimental results, our algorithm demonstrates superior capability in suppressing scattering-induced perturbations compared to benchmark methods, yielding reconstructed images with sharper structural outlines and significantly lower noise levels. From a theoretical perspective, our network architecture explicitly models the scattering process by establishing nonlinear mappings between perturbation modulations and their corresponding degraded outputs. The inherent nonlinear mapping capabilities of neural networks, combined with self-adaptive learning mechanisms, enable dynamic adjustment of reconstruction strategies based on input-specific scattering patterns. This adaptability fundamentally enhances robustness against spatially and temporally varying scattering conditions.

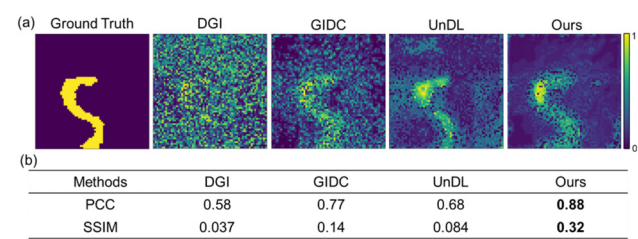


FIG. 6. Experimental results of imaging through rotating diffusers with an average rotation speed of about 2.5°/s. (a) The ground truth and the results reconstructed by DGI, GIDC, UnDL, and our proposed algorithm, respectively. (b) PCC and SSIM values of DGI, GIDC, UnDL, and our proposed algorithm, respectively.

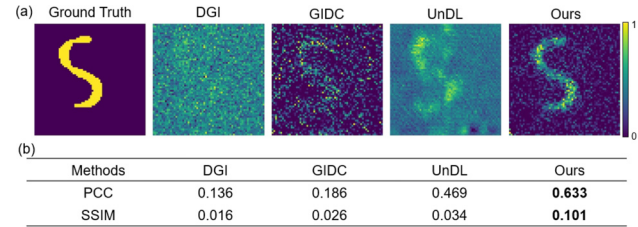


FIG. 7. Experimental results of imaging through rotating diffusers with an average rotation speed of about 5.5°/s. (a) The ground truth and the results reconstructed by DGI, GIDC, UnDL, and our proposed algorithm, respectively. (b) PCC and SSIM values of DGI, GIDC, UnDL, and our proposed algorithm, respectively.

Furthermore, to further evaluate the impact of increasing the rotation speed on imaging quality, we increased the rotation speed to approximately 5.5°/s while keeping the same scattering medium and target. The results are shown in Fig. 7. The reconstruction results of other comparison methods (DGI, GIDC, and UnDL) have become indistinguishable, while our method can still distinguish the letter “S,” which further demonstrates the applicability and robustness of our method compared with other methods in high-speed dynamic scattering scenarios.

Additionally, we measure the computational time of reconstruction algorithms under identical hardware configurations: TGI requires 0.0831 s, DGI needs 0.1771 s, while our method consumes 4.2998 s. The aforementioned work is implemented using the PyTorch-2.6.0 framework on a workstation equipped with an NVIDIA GTX2080 Ti GPU. Although traditional algorithms have an edge in computational speed, they are unable to reconstruct target images. In contrast, neural networks, despite the limitation of slower computational speed, are capable of producing high-quality reconstruction results. Notably, our untrained network demonstrates outstanding generalization performance when dealing with unknown scattering media. In future work, we will commit to shortening the algorithm time to achieve imaging through scattering media with a higher dynamic range.

The proposed method enhances image quality in multiple aspects and achieves image reconstruction in unfamiliar scenarios. First, the proposed methodology primarily leverages the powerful feature extraction capabilities of convolutional neural networks to enable significant enhancement of imaging quality in scattering media environments. We embed the physical model into the neural network, enabling image reconstruction without the need for pre-training. This untrained approach avoids the generalization issues faced by traditional data-driven deep learning methods. Second, we simultaneously input the collected 2D image signals and the computed 1D intensity signals into the network. This allows the network to learn the correlation between these two signals, thereby enhancing model stability. Additionally, complementary information facilitates faster learning convergence. Due to the powerful data-mining and mapping capabilities of deep neural networks, reliable generalization results can be obtained through unknown scattering media. The imaging quality of the physics-informed learning method is also related to various factors, such as the number of training networks, the network structure used, and hyperparameters, which may be directions for future improvement.

In conclusion, we propose an algorithm for imaging through unknown scattering media that simultaneously leverages both

one-dimensional temporal intensity fluctuations and two-dimensional speckle spatial information, enabling high-quality imaging in challenging scattering environments. Our approach incorporates a self-supervised neural network designed to model the transmission matrix, which facilitates the accurate reconstruction of target objects by precisely mapping scattering processes that coexist in both forward and backward directions relative to the target. Experimental results confirm the effectiveness of the proposed method, showcasing its capability to reconstruct target objects with high accuracy and robustness. This method provides valuable insights into advancing imaging techniques in strongly scattering media, laying the foundation for further research and practical applications in this domain.

This work was supported by the Innovation Program for Quantum Science and Technology (2021ZD0300703), the Shanghai Municipal Science and Technology Major Project (2019SHZDZX01), and the National Natural Science Foundation of China (No. 62471289).

AUTHOR DECLARATIONS

Conflict of Interest

The authors have no conflicts to disclose.

Author Contributions

Zhengqing Gao: Conceptualization (equal); Data curation (equal); Formal analysis (equal); Methodology (equal); Writing – original draft (equal). **Xiaoyan Wu:** Funding acquisition (equal); Project administration (equal); Supervision (equal); Writing – review & editing (equal). **Xinliang Zhai:** Conceptualization (equal); Supervision (equal); Writing – review & editing (equal). **Ze Zheng:** Formal analysis (equal); Resources (equal); Writing – review & editing (equal). **Jianhong Shi:** Funding acquisition (equal); Investigation (equal); Supervision (equal). **Jingzheng Huang:** Investigation (equal); Resources (equal); Supervision (equal). **Guihua Zeng:** Funding acquisition (equal); Investigation (equal); Resources (equal); Supervision (equal).

DATA AVAILABILITY

The data that support the findings of this study are available from the corresponding authors upon reasonable request.

REFERENCES

- X. Li, H. Hu, L. Zhao, H. Wang, Y. Yu, L. Wu, and T. Liu, "Polarimetric image recovery method combining histogram stretching for underwater imaging," *Sci. Rep.* **8**(1), 12430 (2018).
- M. Jian, X. Liu, H. Luo, X. Lu, H. Yu, and J. Dong, "Underwater image processing and analysis: A review," *Signal Process. Image Commun.* **91**, 116088 (2021).
- Y.-T. Peng and P. C. Cosman, "Underwater image restoration based on image blurriness and light absorption," *IEEE Trans. Image Process.* **26**(4), 1579–1594 (2017).
- K. Liu, Z. Ye, H. Guo, D. Cao, L. Chen, and F.-Y. Wang, "FISS GAN: A generative adversarial network for foggy image semantic segmentation," *IEEE/CAA J. Autom. Sin.* **8**(8), 1428–1439 (2021).
- G. Satat, M. Tancik, and R. Raskar, "Towards photography through realistic fog," In *IEEE International Conference on Computational Photography (ICCP)* (IEEE, 2018).
- X. Dang, N. M. Bardhan, J. Qi, L. Gu, N. A. Eze, C.-W. Lin, S. Kataria, P. T. Hammond, and A. M. Belcher, "Deep-tissue optical imaging of near cellular-sized features," *Sci. Rep.* **9**(1), 3873 (2019).
- B. Y. Feng, H. Guo, M. Xie, V. Boominathan, M. K. Sharma, A. Veeraraghavan, and C. A. Metzler, "NeuWs: Neural wavefront shaping for guide-star-free imaging through static and dynamic scattering media," *Sci. Adv.* **9**(26), eadg4671 (2023).
- S. Yoon, M. Kim, M. Jang, Y. Choi, W. Choi, S. Kang, and W. Choi, "Deep optical imaging within complex scattering media," *Nat. Rev. Phys.* **2**(3), 141–158 (2020).
- S. Gigan, O. Katz, H. B. De Aguiar, E. R. Andresen, A. Aubry, J. Bertolotti, E. Bossy, D. Bouchet, J. Brake, S. Brasselet *et al.*, "Roadmap on wavefront shaping and deep imaging in complex media," *J. Phys. Photonics* **4**(4), 042501 (2022).
- Y. Jauregui-Sánchez, H. Penketh, and J. Bertolotti, "Tracking moving objects through scattering media via speckle correlations," *Nat. Commun.* **13**(1), 5779 (2022).
- V. Cecconi, V. Kumar, A. Pasquazi, J. S. Toterogongora, and M. Peccianti, "Nonlinear field-control of terahertz waves in random media for spatiotemporal focusing," *Open Res. Europe* **2**, 32 (2023).
- L. Leibov, A. Ismagilov, V. Zalipae, B. Nasedkin, Y. Grachev, N. Petrov, and A. Tsytkin, "Speckle patterns formed by broadband terahertz radiation and their applications for ghost imaging," *Sci. Rep.* **11**(1), 20071 (2021).
- V. Cecconi, V. Kumar, J. Bertolotti, L. Peters, A. Cutrona, L. Olivieri, A. Pasquazi, J. S. Toterogongora, and M. Peccianti, "Terahertz spatiotemporal wave synthesis in random systems," *ACS Photonics* **11**(2), 362–368 (2024).
- J. Bertolotti, E. G. Van Putten, C. Blum, A. Legendijk, W. L. Vos, and A. P. Mosk, "Non-invasive imaging through opaque scattering layers," *Nature* **491**(7423), 232–234 (2012).
- P. Barthelemy, J. Bertolotti, and D. S. Wiersma, "A Lévy flight for light," *Nature* **453**(7194), 495–498 (2008).
- J. Xiong, Z.-H. Zhang, Z. Li, P. Zheng, J. Li, X. Zhang, Z. Gao, Z. Wei, G. Zheng, S.-P. Wang *et al.*, "Perovskite single-pixel detector for dual-color metasurface imaging recognition in complex environment," *Light* **12**(1), 286 (2023).
- S. Li, M. Deng, J. Lee, A. Sinha, and G. Barbastathis, "Imaging through glass diffusers using densely connected convolutional networks," *Optica* **5**(7), 803–813 (2018).
- Y. Li, Y. Xue, and L. Tian, "Deep speckle correlation: A deep learning approach toward scalable imaging through scattering media," *Optica* **5**(10), 1181–1190 (2018).
- Y. Peng and W. Chen, "Deep learning-enhanced ghost imaging through dynamic and complex scattering media with supervised corrections of dynamic scaling factors," *Appl. Phys. Lett.* **124**(18), 181104 (2024).
- X. Zhai, X. Wu, Y. Sun, J. Shi, and G. Zeng, "Anti-noise computational imaging using unsupervised deep learning," *Opt. Express* **30**(23), 41884–41897 (2022).
- F. Wang, C. Wang, M. Chen, W. Gong, Y. Zhang, S. Han, and G. Situ, "Far-field super-resolution ghost imaging with a deep neural network constraint," *Light* **11**(1), 1 (2022).
- T. B. Pittman, Y. H. Shih, D. V. Strekalov, and A. V. Sergienko, "Optical imaging by means of two-photon quantum entanglement," *Phys. Rev. A* **52**(5), R3429 (1995).
- F. Ferri, D. Magatti, L. A. Lugiato, and A. Gatti, "Differential ghost imaging," *Phys. Rev. Lett.* **104**(25), 253603 (2010).
- J. Xu, H. Ruan, Y. Liu, H. Zhou, and C. Yang, "Focusing light through scattering media by transmission matrix inversion," *Opt. Express* **25**(22), 27234–27246 (2017).
- N. Garcia and A. Z. Genack, "Crossover to strong intensity correlation for microwave radiation in random media," *Phys. Rev. Lett.* **63**(16), 1678 (1989).
- O. Ronneberger, P. Fischer, and T. Brox III, "U-net: Convolutional networks for biomedical image segmentation," in *Medical Image Computing and Computer-Assisted Intervention–MICCAI 2015: 18th International Conference, Munich, Germany, proceedings, Part II* (Springer, 2015), pp. 234–241.
- I. Cohen, Y. Huang, J. Chen, and J. Benesty, "Pearson correlation coefficient," *Noise Reduction in Speech Processing* (Springer, 2009).
- Z. Wang, A. C. Bovik, H. R. Sheikh, and E. P. Simoncelli, "Image quality assessment: From error visibility to structural similarity," *IEEE Trans. Image Process.* **13**(4), 600–612 (2004).